energies

Article

Analysis of the Gear Pump's Acoustic Properties Taking into Account the Classification of Induction Trees

Piotr Osiński [1], Adam Deptuła [2,*] and Anna M. Deptuła [2]

[1] Faculty of Mechanical Engineering, Wroclaw University of Science and Technology, 7/9 Łukasiewicza St., 50-370 Wrocław, Poland; piotr.osinski@pwr.edu.pl
[2] Faculty of Production Engineering and Logistics, Opole University of Technology, 76 Prószkowska St., 45-758 Opole, Poland; an.deptula@po.edu.pl
* Correspondence: a.deptula@po.edu.pl; Tel.: +48-511-831-346

Abstract: This paper presents an analysis of selected acoustic properties of gear pumps. For this purpose, the characteristics of selected types of displacement pumps—gear pumps—are discussed, as well as discrete methods of identification and classification of acoustic signals. The basic assumptions of noise analysis in reverberation chambers are discussed, and an analysis of the distribution of measurement points using decision trees and statistical analysis of measured noise levels was conducted. The object for the conducted research was a gear pump with a undercut tooth profile developed by Wytwórnia Pomp Zębatych Sp. z o.o. in Wrocław. Our own research indicates that the acoustic performance of gear units depends on a number of factors, including, in particular, the technology and quality of manufacture and the geometric parameters of the toothing. The aim of the analyses presented in this paper was to determine which of the microphones has the most important impact on the level of determined measured noise generated in the acoustic chamber. The paper presents an analysis aimed at ranking the importance of eight measurement points in which the microphones are located. To this end, induction trees were developed, and a statistical analysis of the measurement results obtained for selected frequency and sound pressure ranges was prepared. The analysis made it possible to optimize the arrangement of microphones in the chamber without unnecessary analysis of each of the microphones separately.

Keywords: gear pump; acoustic properties; induction decision trees; optimization

Citation: Osiński, P.; Deptuła, A.; Deptuła, A.M. Analysis of the Gear Pump's Acoustic Properties Taking into Account the Classification of Induction Trees. *Energies* **2023**, *16*, 4460. https://doi.org/10.3390/en16114460

Academic Editors: Radu-Emil Precup, Ryszard Dindorf, Jakub Takosoglu and Piotr Wos

Received: 23 March 2023
Revised: 19 May 2023
Accepted: 25 May 2023
Published: 31 May 2023

1. Introduction—Theoretical Framework

Excessive noise in the workplace is currently the factor that poses the greatest threat to the life and health of employees. Not only does it cause significant discomfort but it also affects the team's productivity and contributes to errors in tasks performed. Therefore, underestimating acoustic insulation is detrimental to both staff and company performance. Employees in production plants are particularly vulnerable to the harmful effects of noise. Loud machines, open spaces, noise, and frequent movement of workers, vehicles, and materials make halls places where unwanted sounds are difficult to control. However, by using appropriate acoustic solutions, it is possible to significantly reduce reverberation time, separate quieter zones, or properly isolate administrative areas. The basis for all implementation is detailed measurement and determining the standards established by the State Labor Inspectorate to be met. The results of studies presented in, for example [1–3], showed that the use of computer simulation tools to simulate acoustic phenomena in industrial halls is currently the basic and indispensable solution for the effective design of antinoise protection at workstations. The use of simulation methods aims to determine the impact of individual sound sources on the total noise observed at a given workstation, thus identifying the sources responsible for the observed acoustic state. In particular, a very important element is the acoustic diagnosis of machines. In order to analyze the current technical condition of machines, a diagnosis based on measuring the intensity of the vibroacoustic system signal is carried out. In this way, it is possible to observe the appearance of signals indicating a malfunction, such as a drive failure, which can lead to mechanical damage. Another method is the instantaneous sound pressure value [4,5]. The accumulated knowledge thus far indicates certain difficulties in extracting useful signals from the background of the acoustic characteristics of the machine due to the significant contribution of environmental frequency components and the low amplitude values of diagnostic harmonics caused by a given type of damage [6–8].

Machines and devices with hydrostatic drive are widely used in various branches of industry and economy, being found in both stationary and mobile systems. Development of transport would not be possible without hydrostatic systems. Hydraulic systems are used in motor vehicles as well as in water transport and aviation. At the heart of any hydraulic system is the fluid stream energy generator, commonly referred to as a pump [9–12]. It is estimated that more than half (approx. 60%) of the positive displacement pumps produced are external gear pumps [10,13]. These pumps in particular are installed in systems where the energy generator of the fluid stream is characterized by constant efficiency. Gear pumps have numerous operational advantages and low manufacturing costs. The main operating advantages include high durability, high efficiency, operational reliability, resistance to contamination of the working medium, small dimensions due to a simple and compact design, high operating pressures. and a wide range of outputs. Gear pumps have many advantages but generally give way to other pumps from the group of positive displacement pumps [14].

The placement of microphones in a reverberation chamber can be subject to innovation in acoustic measurements. Traditionally, microphone placement in a reverberation chamber is based on evenly spacing the microphones around the source point or along the chamber walls. One innovation in this area is the utilization of advanced microphone placement techniques, which can bring benefits in terms of measurement accuracy and error reduction. Some of these innovative methods are as follows:

Adaptive microphone placement method: This method involves dynamically adjusting the microphone placement based on the measurement characteristics. Adaptive algorithms can optimize the microphone positions in real time, with factors such as the source location, background noise level, and other factors being considered to achieve the best measurement quality.

Nonuniform microphone placement method: In contrast to the traditional uniform microphone placement, the nonuniform placement method introduces intentional irregularities in the microphone array configuration. This can include uneven spacing or variations in distances between microphones. Such nonuniform placement can help reduce interference effects and other disturbances, improving the quality and accuracy of measurements.

Utilization of spatial microphones: Spatial microphones, such as directional microphones or microphone arrays, can be employed as innovative solutions in reverberation chambers. With their ability to selectively capture sound from specific directions, spatial microphones can provide more precise acoustic measurements in specific areas, which is particularly useful for field analysis.

Noisy operation of any device can be reduced by using one of the two methods listed below:

(a) The active method—this method involves interfering with the source and cause of sound-forming vibrations;
(b) The passive method—this method is based on the scattering or absorption of an acoustic wave emitted by a source.

The active method provides the best results (of the two methods mentioned). It is the most costly and time-consuming method, but the most effective. In praxis, the best results are obtained by using two methods simultaneously, both active and passive. Our own research [12,14] and studies from the literature [15] indicate two basic sources of sound-forming vibrations. These are sources that originate from the occurrence of hydraulic and mechanical phenomena. Hydraulic sources include noise caused by the flow of the working medium (fluid-borne noise). On the other hand, mechanical noise is caused by the vibration of structural elements and depends on the quality of manufacture and installation (e.g., unbalanced rotating elements). The leading sources of noise in gear pumps are the pulsation of discharge pressure and the sealing of hydraulic oil during the two-pair meshing of mating gear wheels [15]. These sources contribute the most to the global sound pressure emission level. In order to avoid the formation of obstructed space, relief grooves are made in the slide bearing body, or dampers are mounted on the discharge port to reduce the amplitude of pressure pulsations (the passive method). Passive methods are a kind of half-measure because they focus on the effects of the phenomenon rather than on the cause. A more effective way to reduce the emitted noise is to analyze the cause and employ a method that eliminates the unfavorable phenomenon directly at the source of its formation (the active method). The application of simulation methods aims to determine the influence of individual sound sources on the total noise observed at a given location and thus identify the sources responsible for the observed state. The present paper focuses on the analysis of the acoustic field of a gear pump with an undercut tooth, determining directions and possibilities for improving the pump's operation. In particular, better measurement concepts have been developed as a result of implementing the proposed optimization solutions.

Our basic research indicates that the noise emitted by gear pumps depends on the geometry of the tooth outline, as well as on the technology and class of accuracy of their manufacture [12–14]. It is the geometry of the gear that determines the formation of the obturation space, while the adopted technology and class of manufacturing accuracy affect, among other things, the formation of possible radial run-outs or the formation of backlash. The present study was limited to the analysis of the acoustic parameters of a gear pump prototype with tooth root relief, in particular with the use of game graphs and statistical analysis. The purpose of the analysis was to determine which of the microphones has the greatest impact on the noise level measured (or determined) in the acoustic chamber. Then, it will be possible to develop test guidelines based only on measurement in a reduced number of microphones (optimally in one). First, an induction tree was generated for each of the microphones for the indicated frequencies and sound pressure. On this basis, the importance of individual microphones was determined. In the next stage, a statistical analysis of the collected data was carried out in order to verify the obtained results.

The aim of the current study was to optimize the acoustic properties of a selected gear pump. As part of the research, an analysis of the pump's design parameters was conducted based on measurements of the generated noise. The measurement of noise was considered a key point which depended on the appropriate microphone placement in the chamber. The placement of measurement points is crucial for measurement errors, which can lead to unnecessary design changes. Determining key measurement points allowed for a focus on the so-called narrow necks of the reverberation chamber and, thus, enabled efficient engineering calculations instead as opposed to an analysis of each point separately. For this purpose, two independent analyses were conducted (measured noise level with eight independent measurement points) using decision trees and statistical analysis. The aim of the analysis was to indicate which microphones recorded the most constant noise measurements. The optimized method of considering the microphone signal is expected to yield better measurements of power level Lp and corrected sound power level L_{pA} as a function of discharge pressure pt and pump shaft speed n.

2. Research Object

The prototype pump was made based on early design documentation [12,16,17]. The pump has a three-plate structure. This structure is schematically shown in Figure 1. Mounting holes are made in the faceplate (1) for fixing on the drive unit. The gears, plain bearing housings, and discharge and suction holes are located in the center plate (2). The back plate (3) encloses the entire construction.

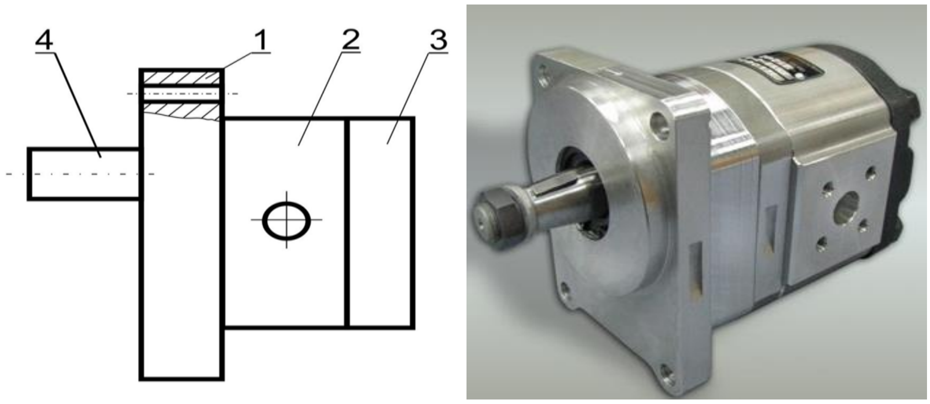

Figure 1. Gear pump with external gearing and a three-plate construction. 1—front (mounting) plate; 2—middle (rest) plate; 3—rear plate; 4—driving shaft.

The prototype pump was designed as part of the company's own research work. The unit was made at the Wytwórnia Pomp Zębatych Sp. z o.o. in Wroclaw. The design of the prototype pump took into account the company's machinery and technological capabilities. The company designed an innovative tooth outline with controlled undercutting of the tooth foot [12,16,17]. The tooth profile of the gear pumps is an involute curve from the undercut point to the tip of the tooth. Below the undercut point, the tooth profile corresponds to an elongated involute curve. The main parameters are summarized in the Table 1 below. The pump hasa unit capacity of q = 40 cm^3.

Table 1. Meshing parameters.

Parameter	Symbol	Unit	Value
Number of teeth	z	-	9
Modulus	m_0	[mm]	4.5
Pressure angle	α_0	[°]	20
Gear wheel width	b	[mm]	32.2

2.1. Measuring Rig

The gear pump along with the capacitive microphones was placed inside an acoustic chamber. The remaining part of the control and measurement equipment was located in a separate room. The isolated room was acoustically separated from the reverberation chamber and was directly adjacent to it. The sound insulation of the partition separating the reverberation chamber from the room containing the measuring equipment was 50 dB.

Acoustic tests were carried out in a reverberation chamber that meets the standards of ANSI S1.21-1972 [18] and standard PN-85/N-01334 [19]. The chamber is used for certification in the area of vibration and noise of machinery and equipment. Isolation from airborne sounds of the chamber is 50 dB in the entire range of audible sounds, i.e., from 20 to 20 kHz. High acoustic insulation from airborne sounds ensures the elimination of interference generated by the propulsion system and by the supercharging hydraulic system. The supercharging system is responsible for ensuring the proper inflow of working fluid to the unit under test [12].

A schematic of the station for measuring vibroacoustic quantities is shown in Figure 2. The pump with the condenser microphones is located inside the reverberation chamber. The rest of the control and measurement apparatus are located in a separate room. Prior to the measurements, the entire measurement path was over-tuned. A reference sound pressure source (pitophone) was used for this purpose.

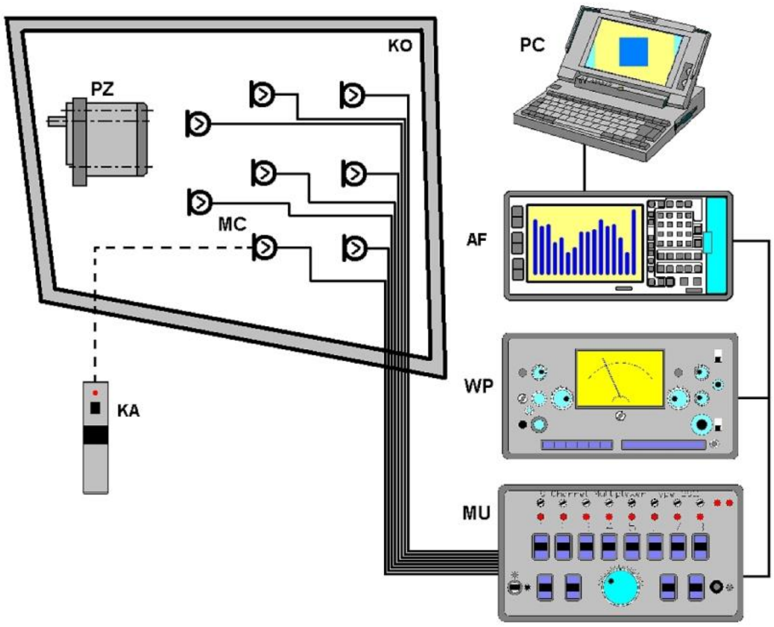

Figure 2. Block diagram of the gear pump noisiness-measuring rig. KA—calibrator; MC—eight free sound field microphones; MU—multiplexer; WP—instrumentation amplifier; AF—two-channel frequency analyzer; PC—computer; PZ—gear pump; KO—chamber.

The reverberant acoustic chamber (Figure 3) consists of two irregular polyhedrons separated by mineral wool. Each of the walls of the polyhedron is made of solid brick, while its internal plasters are made of cement mortar. Having opposite walls at different angles eliminates the formation of standing waves (no pair of opposite walls is parallel to each other). The uniformity of the reverberation field distribution inside the chamber meets the normative requirements, starting from the octave with the center frequency of 125 Hz. Eight fixed measurement points were designated based on the admittance tests. As recommended by the auditor, microphones were placed at each point at the height of the propeller shaft, i.e., 1.3 m above the surface of the floating floor. A multiplexer with a sound level meter was used to read the measured sound pressure level values, and the spectral characteristics were recorded in the storage memory of a two-channel analyzer (Figure 2). The sound pressure levels recorded at the measurement points were averaged. A PC with B&K Type 5306 software was used to analyze the data. Figure 4 shows a gear pump in an acoustic chamber with the attached flow hoses.

Figure 5 shows the test stand for hydraulic testing. Figure 6 shows the microphone in the voice chamber.

Noise generation in gear pumps mainly depends on the manufacturing technology, as well as on parameters such as drive motor speed, suction and discharge pressure, oil viscosity, etc. The frequency and level of oscillatory force in bearings are mainly influenced by the rotational speed and discharge pressure. This results in sound vibrations radiated through the housing to the environment. The working medium supply conditions are determined by the suction pressure. If the suction pressure is too low, a discontinuity in the flow may appear as a result of cavitation causing an increase in the noise level in the mid- and high-frequency bands, i.e., the band in which, from the point of view of human sound perception, noise is perceived as more annoying and troublesome.

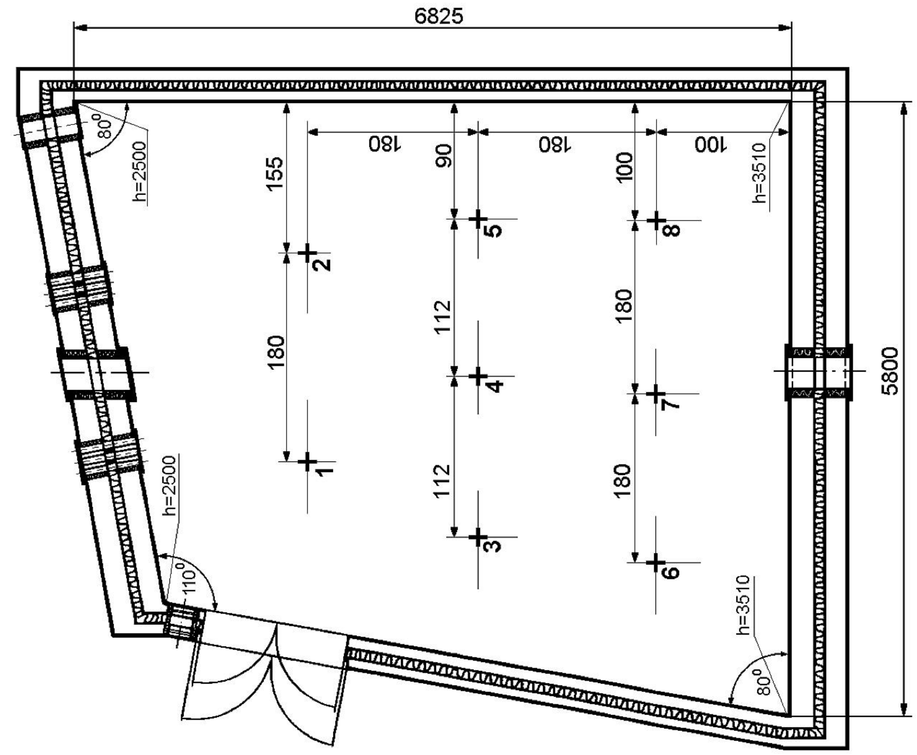

Figure 3. Reverberant acoustic chamber.

Figure 4. A gear pump in the acoustic chamber.

Figure 5. Drive unit located outside the reverberation chamber.

Figure 6. Test stand: acoustic chamber with visible microphones.

For the repeatability of measurement results, the measurement of noise was considered a key point, which depended on appropriate microphone placement in the chamber. The placement of measurement points is crucial for measurement errors, which can lead to unnecessary design changes. Determining key measurement points allowed for focusing on the so-called narrow necks of the reverberation chamber and, thus, enabled efficient engineering calculations as opposed to the analysis of each point separately. For this purpose, two independent analyses were conducted (measured noise level with eight independent measurement points) using decision trees and statistical analysis. The aim of the analysis was to indicate which microphones recorded the most constant noise measurements. The optimized method of considering the microphone signal is expected to yield better measurements of power level *Lp* and corrected sound power level L_{pA} as a function of discharge pressure pt and pump shaft speed *n*.

2.2. Acoustic Research

Initially, the study measured sound pressure level L_m, adjusted sound pressure level L_A, sound power L_p, and adjusted sound power level L_{pA}. The average value of the sound pressure level L_m for the measured points was calculated according to the following formula:

$$L_{\mathrm{m}} = 10\lg\left(\frac{1}{\mathrm{n}}\sum_{\mathrm{i}=1}^{\mathrm{n}} 10^{0.1\mathrm{L}_{\mathrm{mi}}}\right) \quad (1)$$

where L_{mi} is the sound pressure level at *i*-th measurement point, and *n* is the total number of measurement points.

The average value of the corrected A sound level was specified in the same manner:

$$L_A = 10\lg\left(\frac{1}{n}\sum_{i=1}^{n} 10^{0.1L_{Ai}}\right) \quad (2)$$

where L_{Ai} is the sound pressure level at *i*-th measurement point, and *n* is total number of measurement points.

The value of the corrected sound level A was specified from the measured sound pressure level L_m^j in the *j*-th band and after introducing K_{Aj} the correction resulting from the weighted curve characteristics:

$$L_A^j = L_m^j + K_{Aj} \quad (3)$$

where L_m^j is the sound pressure level in the *j*-th frequency band,L_A^j is the corrected sound pressure level in the *j*-th frequency band, and K_{Aj} is the correction according to characteristic *A* for the *j*-th frequency band.

Withthe sound power level L_p, the sound power level L_p and the corrected sound power level L_{pA} were determined as follows:

$$\mathrm{L_p^j} = \mathrm{L_m^j} + 10\lg\frac{\mathrm{A^j}}{\mathrm{A_0}} + 10\lg\frac{1+\frac{\mathrm{S_v}\lambda}{8\mathrm{V}}}{1-\frac{\mathrm{A^j}}{\mathrm{S_v}}} - 6 + \mathrm{C} \quad (4)$$

where L_m^j is the average value of the sound pressure level in the *j*-th frequency band, L_p^j is the average value of acoustic power in the j-th frequency band, A^j is the acoustic absorption in m^2 calculated in the j-th frequency band for the most important microphone, A_0 is 1 m^2,S_v is the area of the chamber with floor, V is the volume of the chamber [m^3], V_0 is 1 m^3, λ is the wavelength including the most important microphone, and C is the correction depending on climatic conditions (for atmospheric pressure of 100 kPa and temperature of 20 °C, C = 0).

The corrected sound power level L_p^j in the j-th frequency band was determined based on the following formula:

$$L_{pA}^j = L_{pA}^j + K_{Aj} \quad (5)$$

where L_{pA}^j is the corrected sound power level in the j-th frequency band, and *n* is thetotal number of frequency bands.

Acoustic tests were performed for predetermined operating pressures ranging from 0 to 30 MPa. Readings were taken every 2 MPa. The frequency range included thirds with center frequencies from 25 to 20k Hz. Table 2 presents a summary of exemplary acoustic measurements of a gear pump after tooth root undercutting for p_t = 12 MPa [12,16].

Table 2. Acoustic measurements of a gear pump after tooth root undercutting for pt = 12 MPa [12,16].

f [Hz]	Number of Microphones								Tercje				Oktawy	
	1	**2**	**3**	**4**	**5**	**6**	**7**	**8**	L_{mj}	S_{mj}	K_{Aj}	L_{Aj}	L_{mj}	L_{Aj}
	−1.48	−0.15	−0.20	0.33	0.16	−0.10	0.26	0.42						
25	84.1	81.8	62.5	46.8	65.4	83.8	82.4	78.1	80.1	15.4	−44.7	35.4		
31.5	62.3	60.0	54.9	40.0	56.8	63.7	60.3	62.0	60.1	8.0	−39.3	20.8	80.2	40.9
40	58.9	49.4	58.5	55.7	52.9	51.8	46.4	53.7	54.7	4.3	−34.6	20.1		
50	70.8	67.8	74.2	74.9	73.0	66.0	65.3	62.2	71.1	5.0	−30.2	40.9		
63	71.7	76.4	76.1	75.2	71.9	66.0	78.4	59.6	74.4	6.8	−26.2	48.2	77.1	50.9
80	75.4	73.0	67.1	69.8	64.9	63.8	68.7	69.0	70.1	3.8	−22.5	47.6		
100	69.9	64.8	60.9	61.9	65.4	65.1	60.8	62.8	64.6	2.7	−19.1	45.5		
125	74.6	73.3	75.1	66.6	71.0	66.2	68.5	70.0	71.5	3.3	−16.1	55.4	75.0	58.9
160	69.8	69.1	70.5	69.5	68.6	74.1	71.9	75.1	71.8	2.8	−13.4	58.4		
200	81.8	71.1	76.8	74.0	69.4	78.2	76.5	74.0	76.3	3.8	−10.9	65.4		
250	83.0	72.6	79.8	76.3	73.0	80.2	79.5	75.9	78.4	3.5	−8.6	69.8	81.2	72.6
315	77.1	68.8	73.4	70.6	75.0	72.6	74.0	65.7	73.0	3.5	−6.6	66.4		
400	83.4	80.6	80.2	69.9	69.7	79.6	73.2	74.2	78.2	5.2	−4.8	73.4		
500	84.2	81.3	80.5	71.4	70.8	80.6	74.4	75.1	79.0	4.9	−3.2	75.8	81.9	78.7
630	65.4	67.1	69.4	71.3	73.8	68.2	70.4	71.8	70.5	3.4	−1.9	68.6		
800	60.7	60.9	63.9	62.5	64.1	63.1	69.5	63.8	64.6	3.3	−0.8	63.8		
1k	61.8	63.4	65.9	63.5	63.1	63.4	71.7	65.7	66.2	3.8	0	66.2	71.4	71.4
1.25k	68.8	68.8	71.2	69.7	67.8	66.5	65.8	66.6	68.4	1.8	0.6	69.0		
1.6k	72.5	69.3	68.9	68.1	70.8	70.8	67.1	65.4	69.3	1.9	1	70.3		
2k	72.3	72.0	72.2	70.4	69.6	72.9	71.1	71.3	71.5	0.9	1.2	72.7	74.8	76.0
2.5k	70.2	69.2	70.3	69.2	67.1	68.3	69.3	67.3	68.9	1.0	1.3	70.2		
3.15k	66.2	68.5	67.4	65.9	65.9	66.9	65.0	66.0	66.5	1.1	1.2	67.7		
4k	69.4	69.8	69.7	68.2	66.0	68.9	67.7	67.4	68.4	1.1	1	69.4	71.6	72.6
5k	67.5	65.1	65.2	65.4	62.5	63.5	64.3	63.0	64.6	1.2	0.5	65.1		
6.3k	67.7	64.0	63.1	64.9	63.5	62.5	66.1	63.8	64.6	1.5	−0.1	64.5		
8k	68.6	65.5	65.2	64.3	63.2	65.2	64.2	64.4	65.1	1.1	−1.1	64.0	69.3	68.2
10k	65.5	65.6	63.5	63.1	64.3	63.8	62.9	61.9	63.8	0.9	−2.5	61.3		
12.5k	66.1	63.0	63.2	62.4	61.7	61.9	60.8	62.7	62.8	1.1	−4.3	58.5		
16k	59.6	57.7	56.3	58.3	56.3	54.9	55.0	55.2	56.8	1.4	−6.6	50.2	63.9	57.3
20k	53.2	51.4	49.8	49.3	49.0	47.3	47.7	47.6	49.6	1.6	−9.3	40.3		

All acoustic measurement results for all microphones are presented in Supplementary Materials.

Figure 7 presents a summary of the values of the acoustic power level L_p and corrected acoustic power level L_{pA} as well as acoustic pressure level L_m and corrected acoustic pressure level L_A in the function of discharge pressure p_t at a constant rotational speed of a pump shaft n=1500 rpm.

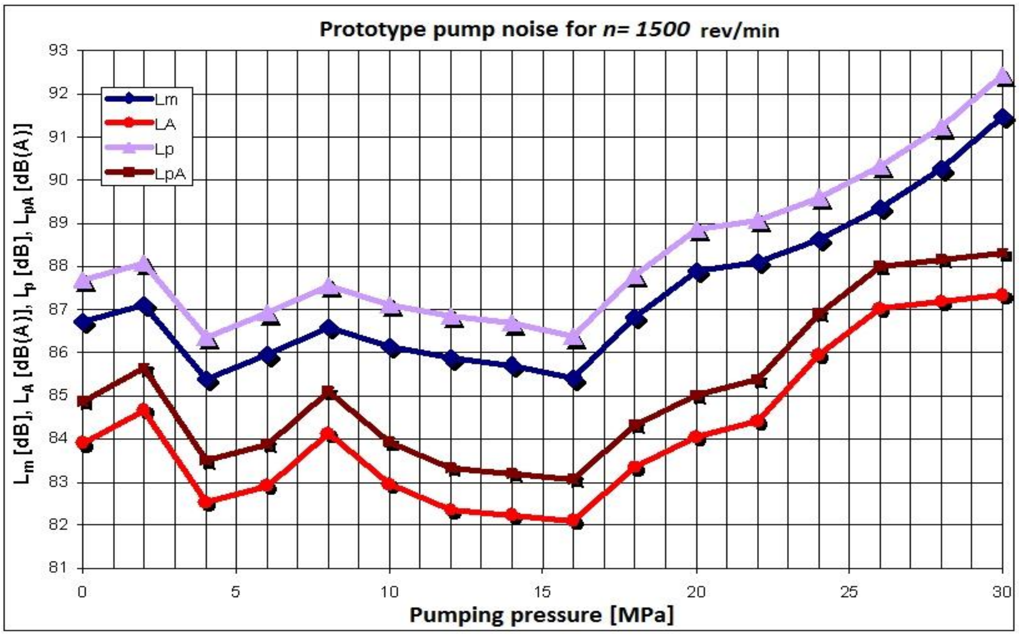

Figure 7. The noise of the experimental gear pump after tooth root undercutting for nominal rpm [12,16].

Figures 8 and 9 present a tertian and an octave spectrum of the gear pump after tooth root undercutting for nominal discharge pressure and nominal rotational speed.

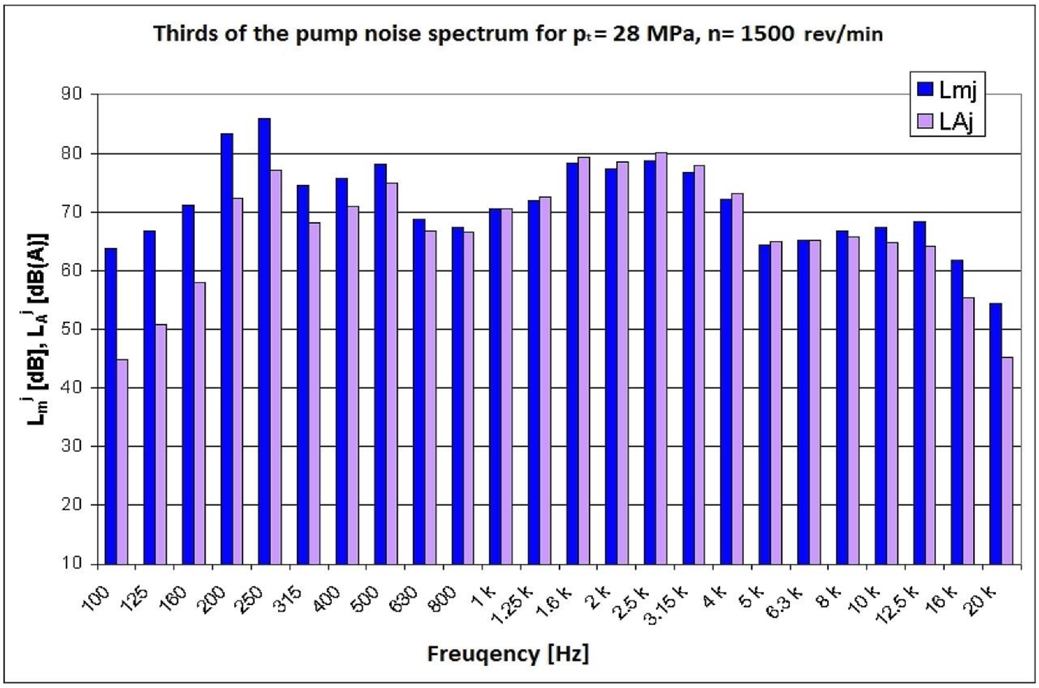

Figure 8. One-third SPL and A sound level spectrum for the experimental unit and for nominal pressure and rotational speed [12,16].

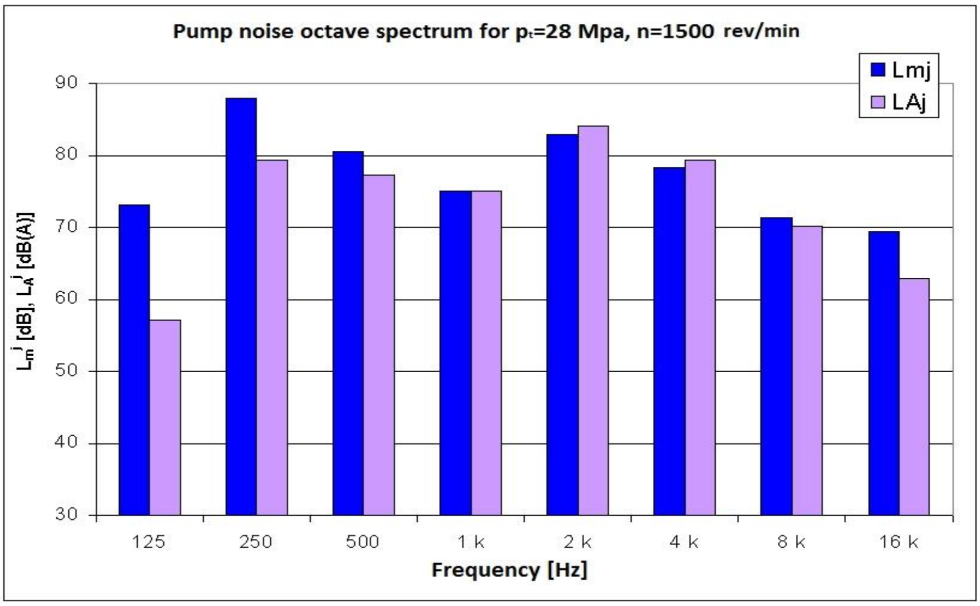

Figure 9. The octave spectrum of an experimental gear unit for nominal pressure and rotational speed [12,16].

Figure 10 compares a corrected level of the acoustic pressure L_A and the corrected level of the acoustic power Lp_A of an experimental unit with undercut tooth root and pump PZ4-32 TKs 186 with a conventional tooth profile.

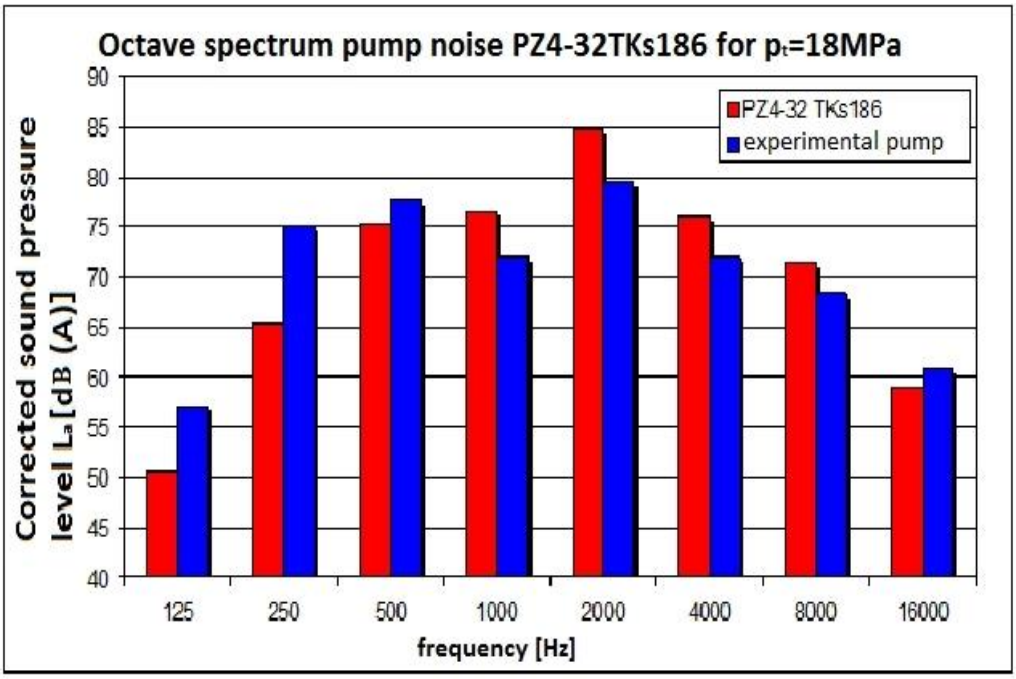

Figure 10. The octave spectrum of an experimental gear unit and pump PZ4-32 TKs 186 [12,16].

In both tested units the teeth of wheels grinding has been made before and after nitriding. In the determined spectrum, the dominant component is an octave with a center frequency of 2k Hz.

A full summary of the obtained data for the experimental pump and PZ4-32 TKs 186 is provided in Table 3. The presented data allow us to assess the effect of modifying the toothed wheels on reducing noise emissions as a function of discharge pressure.

Table 3. Comparison of octaves of the center frequency equal to 2k Hz for an experimental pump and PZ4 TKs 186.

p_t [MPa]	Test Pump $L^{2000}_{A(1)}$	PZ4-32 TKs 186 $L^{2000}_{A(2)}$	ΔL^{2000}_{A}	$10\log(10^{0.1L^{2000}_{A(2)}} - 10^{0.1L^{2000}_{A(1)}})$
6	74.7 [dB]	79.5 [dB]	4.8 [dB]	77.8 [dB]
12	74.8 [dB]	79.5 [dB]	4.7 [dB]	77.7 [dB]
18	78.2 [dB]	83.6 [dB]	5.4 [dB]	82.1 [dB]
24	81.0 [dB]	83.0 [dB]	2.0 [dB]	78.7 [dB]
28	82.9[dB]	83.6 [dB]	0.7 [dB]	75.3 [dB]

3. Discrete Methods of Identification and Classification of Acoustic Signal

Classification has a very important role in the analysis of acoustic properties. According to statistical theory, the propagation of sound energy in a room from the point of view of sound source analysis is of an exponential nature, and its parameter is a constant quantity for a given room—the reverberation time. On the basis of this theory, valid formulas were derived that allow for the calculation of the reverberation time for a given room with a given volume and acoustic absorption—for the analyzed pump. To ensure the high efficiency of the method of classification and identification of objects such as gear pumps based on acoustic signal analysis, it is necessary to take into account as much as possible all the phenomena that affect directly or indirectly the reliable extraction of the correct feature (parameter); that is, the correct (accurate) classification and identification of the object with the highest possible probability. Often, the recognition of acoustic signals is carried out using, for example, the following: [20–25]: HMM (hidden Markov models (vector quantization), LVQ (learning vector quantization), SOM (self-organizing maps), ANN (artificial neural network), GMM (Gaussian mixture model), and SVM (support vector machine) [26,27].

However, in the case of our acoustic pump research, the application of this method for classification will have the following disadvantages:

- Estimating the model can take a long time with a large amount of data.
- Estimating the correct model requires some knowledge.

All machine learning models that use distances (such as the Euclidean metric) or similarities (computed as dot products) between feature vectors require the prior standardization of variables. Methods of neural networks and classification using decision trees are very similar in this regard. However, we decided to use the methodology of decision trees because its fundamental feature is the ability to represent arbitrarily complex concepts. Additionally, compared to other hypothesis representations, decision trees have low memory complexity. Moreover, the computational complexity (assuming that one attribute is tested in one test) is linearly limited by the number of attributes.

In particular, classifications with inductive decision trees or HMMs methods can be used. Hidden Markov models (HMMs) have become a common tool in the last decade for modeling sequences of dependent random variables that can be included in signal classification.

In the first stage of classification analysis, the knowledge base and knowledge source are built. For this purpose, testing and learning files are made. Then, the distribution of proportions between the learning and testing data set is studied, which is needed to determine the classification quality index [28–31].

Figure 11 shows a general acoustic data classification scheme. The sequence of samples as well as the meta record allows for assigning the appropriate classification feature. An important step is also the appropriately correct recording of the resource occupancy management. For this purpose, the algorithm for obtaining the sound intensity must be properly programmed to be used on the computer whose task is to acquire the signal [24,32].

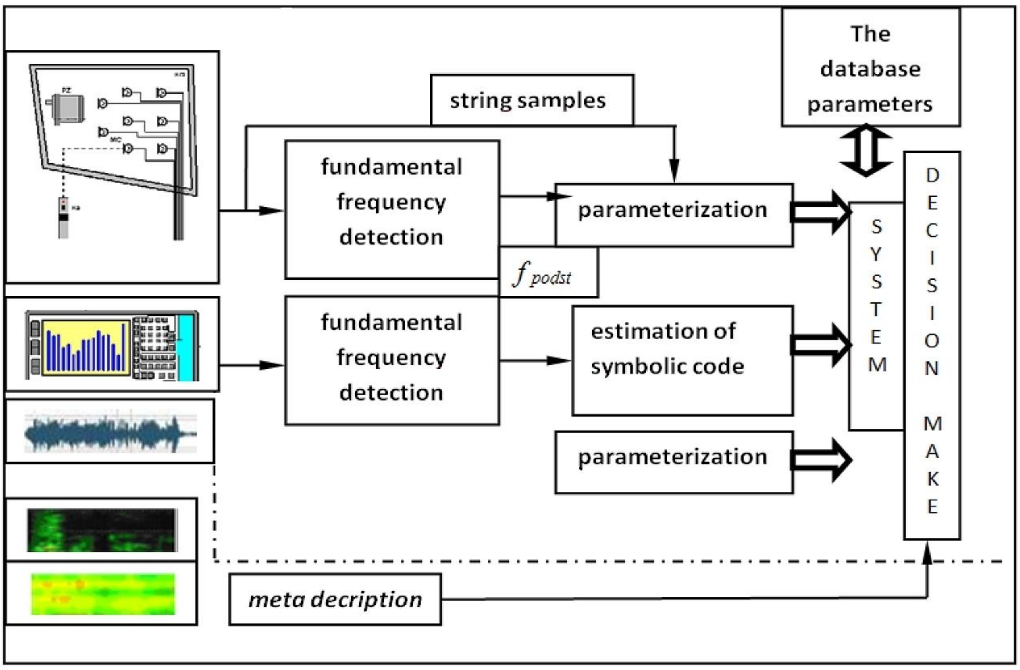

Figure 11. A sample query "query by example" to the decision-making system.

The processof signal analysis using a computerized decision support system can be described in three main steps:

- Time analysis. A special feature of this approach is the departure from the concept of matched filtration and the use of time signal detection;
- Spectral analysis. In particular, the analysis of signals using higher-order cumulants and their spectra enables the study of statistical relationships between the frequency components of the signal, the detection and identification of components resulting from the occurrence of nonlinear phenomena and additional feedbacks, and the reduction of noise in signals.
- Parameterization of the speech signal. This is applied where pattern classification requires a decision as a result of observation of the current feature vector and acquired knowledge (based on the learning set in the learning process).

4. Analysis of Measurement Points

In this section, we describe the application of a decision tree induction algorithm that served as a classifier of acoustic signals. In the first stage of the analysis, data were extracted from previously collected measurements from the real operation of the gear pump. The adopted methodology included the following steps:

1. Data selection—selection of relationships that will be explored and the definition of the method of combining relationships;
2. Data transformation—conversion of attribute types and discretization of continuous values;
3. Knowledge extraction from data—generation of rules and decision trees;
4. Interpretation of results—selection of the most interesting knowledge, logical, and graphical visualization of the results.

The phases of classification and knowledge discovery are schematically presented in Figure 12.

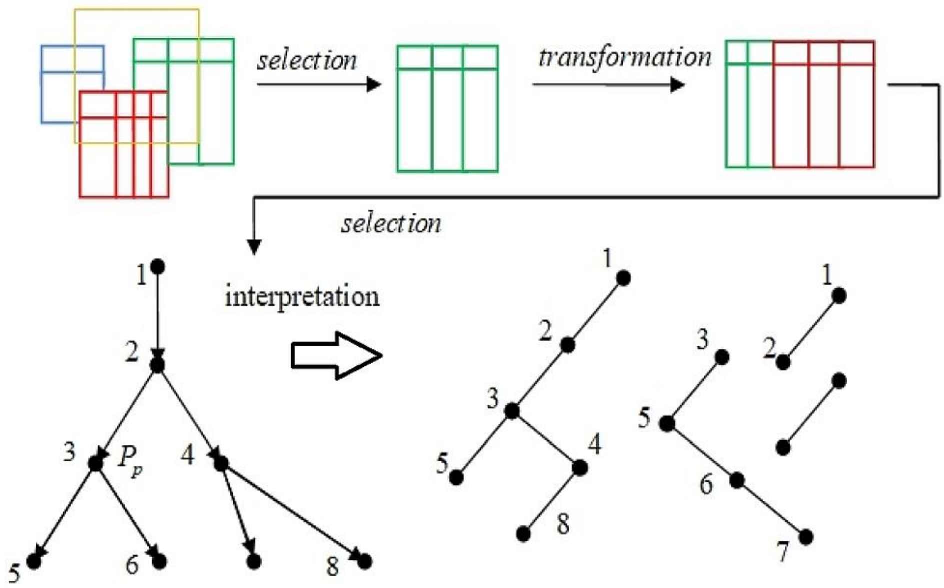

Figure 12. Phases of classification and knowledge discovery.

The initial operation consists of mapping the data into a set of predefined classes. Based on the contents of the database, a model is built (decision tree, logical rules) that serves to classify new objects in the database or to gain a deeper understanding of existing classes. All data relate to acoustic measurements of the examined pump and are listed in their entirety in Supplementary Materials.

4.1. Tree Induction as Classifiers of Acoustic Signals

For this purpose, so-called supervised learning is used. In supervised learning, the learning process concerns the search for hypotheses that describe the so-called concepts. The term concept is understood as "a general term denoting a set (class) of objects having certain common properties that distinguish them from other concepts" [32]. The clustering problem is described as a finite set of k-dimensional vectors: $X = \{x_i\}$, where $i = 1, 2, \ldots, m$.

The clustering operation involves replacing a set of vectors X with a set of classes

$$\Omega = \{\omega_i\}, i = 1, 2, \ldots, \mathrm{n} < \mathrm{m} \tag{6}$$

in such a way that a vector y_i (called prototype) representative of all vectors belonging to the class can be associated with each of ω_i.

If the criterion for the distribution of classes is a certain scalar function F, then the assignment of a x_i vector to a certain class reduces to finding such a distribution of classes that

$$F(\omega_{opt}, x_i) = \mathrm{minF}(\omega_i, x_i) \tag{7}$$

The goal is to extract homogeneous clusters of data; that is, to divide the set X into subsets that meet the conditions of separability and completeness as follows:

$$\omega_i \cap \omega_j = 0 \text{ for } i \neq j \text{ and } \omega_1 \cup \omega_2 \cup \ldots \cup \omega_n$$

After grouping, the next step is classification using the induction algorithm.

The teacher (supervisor) provides examples and counterexamples of the selected concept (also referred to as positive and negative examples). Some authors use the term "category" or "class" instead of "concept". By hypothesis, this is understood as a function that assigns examples to their categories. The result of supervised learning of concepts is the selection of a certain hypothesis from the space of possible hypotheses, which is deemed to best describe the concepts on the basis of the provided learning examples.

In the case of knowledge discovery from data, historical information representing experience in a certain field is stored in a database, and classification of objects acting as examples is often known. In this case, a real teacher pointing to examples is not necessary. If knowledge of the domain is limited and if a known classification of objects is not available, it is it is possible to use data analysis methods, e.g., cluster analysis.

In particular, an inductive knowledge acquisition system based on the concept of entropy can be used [33–35]. They can be divided into three basic categories:

1. Algorithms for minimum rule set induction;
2. Algorithms for the induction of an exhaustive set of rules;
3. Algorithms for the induction of a satisfactory set of rules.

The search for the optimal minimum set of rules is an NP-complete problem [36]. The search for an exhaustive set of all rules is an exponential complexity problem. Creating a satisfactory set of rules requires specifying the constraints that must satisfy the rules. They refer to the user's acceptability of the values of the selected rule evaluation measures. Such a set of rules can be generated from a set of all rules and then filtered to find interesting rules.

Decision Rules in the Classification of New Objects

Rule induction is performed on a training dataset $DT = (U, A \cup \{d\})$ in which U is a finite set of objects (records) characterized by a set of features (conditional attributes) A and a decision attribute d. In our analysis, the objects are microphones, while the attributes are acoustic parameters.

Each attribute $a_k \in A$ is treated as a function $a : U \rightarrow D_a$, where D_a is the range of the attribute.

That is, ultimately, we have $\{a_1, \ldots, a_k\} \subseteq A$, $V_{ai} \subseteq D_{a_i}$ and $v_d \in D_d$. There is $a \in A$ then a so-called directional descriptor. A set of objects with identical values of a decision attribute is called a decision class. Induction of rules on the basis of the data contained in the training table can be performed using various algorithms that generate both so-called minimum decision rules and using the sequential overlap method.

All algorithms use certain measures that determine either the form of the rule to be determined or which of the rules already determined can be removed or combined.

In the prediction perspective, decision rules generated from learning examples are used to classify new objects, which are objects that were not used for induction. Their description by means of attribute values is known while the purpose of their classification is to determine the assignment of such an object to a decision class. In addition, if the actual classification of classified object is known, then it is called a test case because it is then possible to compare the prorated classification decision with the actual one. Object classification is based on matching the description of the object to the parts of the conditional decision rules. We distinguish between complete and partial matching. The complete matching of an object to the conditional part of a rule is described by Formulas (6)–(9)

If any attribute is not specified, it is most often assumed that an object can take any value from the domain of that attribute when matching a rule. Complete matching of object e to the conditional part of rule r, occurs with the following:

$$\forall ai \in Cr(f(ai, e) \propto term(ai)) \tag{8}$$

In the case of rule syntax consistent with (2):

$$(f(d, x) = jvd) \tag{9}$$

where the conditional part P is the conjunction of the conditions ($f(ai,x) = vai$), and the decision attribute d takes values from the domain Vd. In generalizations of approximate sets, the notation is simplified to the following:

$$(f(ai,e) = vai) \tag{10}$$

where the conditional part P is the conjunction of the conditions($f(ai,x) = vai$), and the decision attribute d takes values from the V_d domain. Partial matching of object e to the conditional part of rule r occurs when there is at least one attribute $aj \in Cr$, for which the following condition is not satisfied:

$$(f(aj,e) \propto term(aj)) \tag{11}$$

The matching of decision rules to the description of the classified example is implemented differently depending on whether the decision rules are ordered in the form of a decision list or form an unordered set of rules. In the case of a decision list, the matching of an object to subsequent rules in the list is performed [36,37].

The suitability of a set of rules for classifying new objects is evaluated by estimating the classification error or classification accuracy with respect to a set of test examples whose class membership is determined. The distribution of examples is assumed to be random and representative. Many decision rule induction algorithms are used in knowledge discovery.

4.2. Classification Based on Conditional Entropy Minimization

This is a method that uses a measure of entropy. For the considered set of examples S and attribute a, entropy is defined as

$$Ent(S) = -\sum_{i=1}^{r} p_i \cdot \lg_2 p_i \tag{12}$$

where p_i is the probability of a given class.

Any boundary point ca divides the binary set S into two disjoint subsets S_1 and S_2 ($S = S_1 \cup S_2$). For such a division, the conditional entropy is defined as follows:

$$\frac{|S_1|}{|S|} \cdot Ent(S_1) + \frac{|S_2|}{|S|} \cdot Ent(S_2) \tag{13}$$

For a given attribute a, the boundary point is selected that minimizes the value of the conditional entropy. Attribute a values should be sorted before analysis.

The work implements a decision tree induction algorithm that uses entropy gain to evaluate potential splits of nodes while simplifying the tree during its construction.

The inductive decision tree consists of the following:

- A root containing all training samples;
- Nodes having a single feature or a set of features from the training samples;
- Leaves—the data from the training samples ultimately ranked according to certain features.

Creating a tree starts with deciding what will be a leaf and what will be a node and choosing a category or test label for it. If a node has been created, then the individual results correspond to branches leading from this node to subtrees constructed according to the same scheme. The creation of a tree begins with deciding what will be a leaf and what will be a node and selecting a category or test label for it.

The expected value of information after the division of the set of examples E into subsets $E^{(m)}$, $m = 1, \ldots, |V_a|$, for which the attribute a has the value V_m, is determined as

$$I(E,a) = \sum_{m=1,K,|V_a|,E^{(m)}=\varnothing} \frac{\left|E^{(m)}\right|}{|E|} \cdot I\left(E^{(m)}\right) \tag{14}$$

where $\left|E^{(m)}\right|$ is the number of examples after the division of the set E in relation to the value m of a given attribute, and $|E|$ is the number of examples in the training set E.

$$I(E) = -\sum_{i=1}^{|E|} \frac{|E_i|}{|E|} \cdot \log_2\left(\frac{|E_i|}{|E|}\right) \tag{15}$$

Then, classification is carried out using trees separately for sound pressure *Lm*, frequency kHz, and discharge pressure MPa as output attributes (wy): *Lm*(wy), kHz (wy), and MPa (wy).

Input attributes (we) are the values of acoustic measurements registered from eight microphones: *microphone 1* (we), *microphone 2* (we), *microphone 3* (we), *microphone 4* (we), *microphone 5* (we), *microphone 6* (we), *microphone 7* (we), and *microphone 8* (we).

The basic characteristic that characterizes the efficiency of decision algorithms is the ability to generate decision trees. The generated trees allow for rule induction, which leads to the creation of a training table.

Calculation steps:

1. Calculate the entropy for each attribute;

2. Select attribute A with the lowest entropy;

3. Divide the set of learning examples due to the value of attribute A into disjoint subsets;

4. Add edges to the tree with the following conditions:

If A=a1 then … (subtree 1);

If A=a2 then … (subtree 2).

…

5. For each subtree, perform the steps from 1;

6. In each iteration, one attribute is removed, and the algorithm stops, when there is no attribute left to consider or all examples in a given subtree have the same decision attribute value.

As a result of the analysis, induction trees were generated for each parameter *Lmj*, p_t [MPa], and *f* [Hz] (Figures 13 and 14).

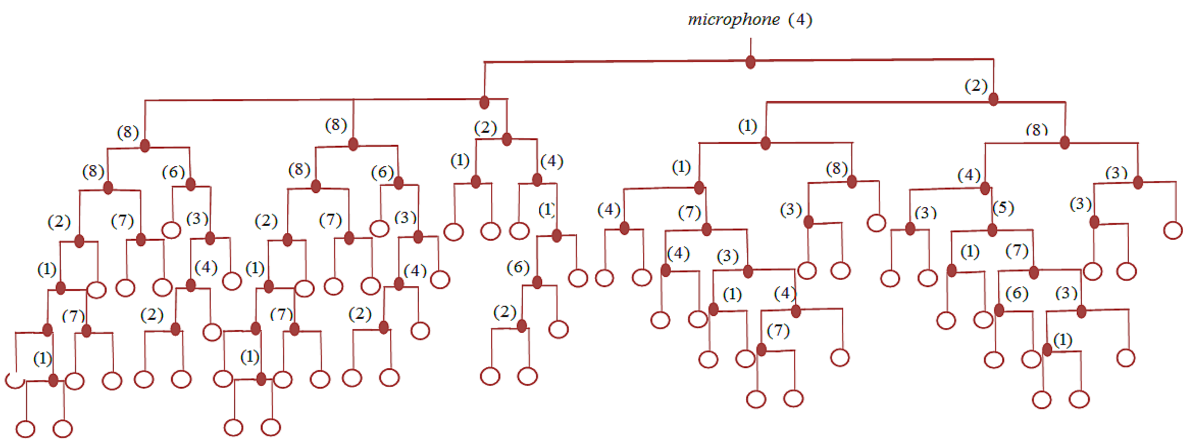

Figure 13. A simplified induction tree for the discharge pressure *pt* [MPa] for microphone 4, the number of examples forming tree graph-4, and tree trimming 25%.

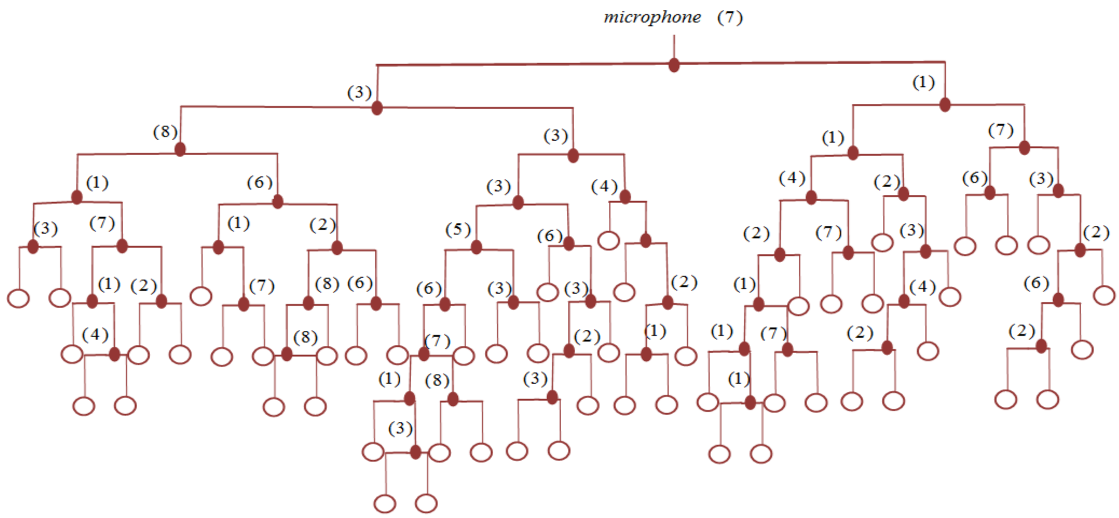

Figure 14. A simplified induction tree for the frequency f [Hz] for microphone 7, the number of examples forming the tree graph4, and tree trimming 40%.

The induction tree ranks the degree of importance of an attribute from the most important one located at the root.

The most important acoustic signal generated by the outlet pressure value occurs at microphone 4 according to the tree in Figure 13, while the most important acoustic signal influenced by the frequency change is generated at microphone 7 according to the tree in Figure 14. The most important signal influencing the acoustic pressure value is the one recorded at microphone 7.

Depending on how the input array (data from measurements) is divided into a training and test array, different classification accuracy values can be obtained. Therefore, we applied statistical analysis, which allowed us to determine a reliable estimator of the classification accuracy coefficient. This enables us to analyze the rank of importance of microphones.

5. Initial Statistical Analysis

The statistical analysis described in this section function as an additional selection of possible solutions [38–40]. A possible solution is understood as that which determines which of the measuring points has the greatest impact on the measured sound pressure values. The analysis was conducted for each microphone separately. The aim of the analysis was to indicate which microphones recorded the most constant noise measurements.

First, a preliminary statistical analysis of registered noise levels for each of the preset frequencies was performed. As part of the preliminary analysis of descriptive statistics, the mean X, the standard deviation S, and the coefficient of variation V were compared for each variable represented by the particular frequency bands applied in the study. The investigated cases (15 cases) were based on the measurement values obtained for subsequent pressure values 0, 2, 4, . . . , 30 [MPa].

The obtained results for the indicated characteristics are presented in Tables 4 and 5.

The green frames in Figure 15 represent, for each of the microphones, the hierarchy resulting from the analysis of the minimum mean value of registered noise (for all analyzed instances). The hierarchy resulting from the analysis of the maximum recorded noise value is presented in the red boxes. The analysis shows that the minimum average noise value of 42.11 dB was recorded on microphone 4. The lowest average value from the maximum recorded noise is 76, which was recorded by microphone 5. We can also mention microphone 7, which was found to be exactly seventh in the hierarchy of minimum and maximum noise levels.

The following parameter applied in the analysis involved the coefficient of variation. The interpretation of the resulting coefficients of variation indicated that the most constant measurements were recorded using microphone 6, where $Vmin1 = 0.92$ and microphone 1, for which case $Vmax1 = 8.97$. In turn, microphones 3 and 8 were characterized by the biggest values in terms of the obtained coefficient of variation, respectively.

Table 4. Summary of mean values, standard deviation, and variability coefficient for microphones 1–4 for the examined frequencies.

	Number of Microphones 1–4											
	1			2			3			4		
f [Hz]	**X**	**S**	**V**	**X**	**S**	**V**	**X**	**S**	**V**	**X**	**S**	**V**
25	81.16	4.97	6.12	82.22	4.49	5.46	66.62	2.72	4.09	59.37	3.27	5.50
31.5	62.46	2.35	3.76	60.62	3.74	6.16	58.61	2.67	4.56	42.11	1.12	2.66
40	59.59	1.82	3.05	49.93	0.78	1.56	56.38	1.49	2.64	53.75	1.65	3.06
50	66.23	4.07	6.15	66.38	1.69	2.55	70.84	1.68	2.37	71.51	1.94	2.72
63	73.61	1.75	2.37	74.99	1.82	2.42	75.24	1.74	2.32	75.77	1.19	1.57
80	70.72	2.77	3.91	71.03	2.48	3.49	67.48	1.83	2.71	70.33	1.90	2.71
100	67.66	2.23	3.30	62.87	1.51	2.40	61.38	1.60	2.61	63.39	1.67	2.63
125	70.98	4.16	5.86	68.86	2.79	4.04	72.53	2.82	3.89	65.84	1.88	2.86
160	67.89	1.66	2.44	69.52	2.62	3.77	70.93	1.58	2.22	69.57	1.49	2.15
200	80.12	4.87	6.08	74.86	4.20	5.61	76.98	3.62	4.70	77.73	5.04	6.49
250	82.01	4.34	5.29	76.17	4.24	5.57	80.13	3.10	3.88	79.41	5.35	6.73
315	73.78	2.83	3.84	67.81	1.44	2.13	71.97	1.90	2.64	70.20	2.03	2.89
400	80.11	2.95	3.69	79.41	4.35	5.48	76.84	4.78	6.23	73.95	3.27	4.43
500	81.31	3.04	3.74	80.24	4.32	5.38	77.76	4.57	5.88	75.34	3.29	4.37
630	69.56	4.03	5.79	67.79	3.61	5.33	66.93	3.30	4.93	68.40	3.73	5.46
800	65.34	3.07	4.69	63.88	4.79	7.50	64.03	2.42	3.78	64.55	3.94	6.10
1k	66.74	3.49	5.23	65.86	5.91	8.97	66.66	2.81	4.21	66.60	4.54	6.81
1.25k	70.30	2.06	2.93	68.85	1.99	2.89	70.28	2.67	3.80	69.33	1.81	2.60
1.6k	74.98	3.73	4.97	73.24	3.62	4.94	71.40	3.77	5.29	73.59	4.51	6.13
2k	74.27	2.93	3.95	73.26	3.47	4.74	73.13	2.86	3.91	72.07	2.69	3.73
2.5k	72.44	4.58	6.33	71.50	5.57	7.80	70.75	4.45	6.29	70.88	4.68	6.60
3.15k	70.34	5.11	7.27	70.03	5.13	7.33	68.64	4.65	6.77	69.99	5.13	7.33
4k	70.25	2.75	3.92	69.83	2.65	3.80	69.36	2.32	3.34	68.86	2.41	3.50
5k	67.28	1.45	2.16	66.21	2.30	3.47	65.27	1.77	2.71	65.55	1.51	2.30
6.3k	64.71	2.15	3.32	63.89	2.58	4.04	62.36	2.18	3.50	62.32	2.17	3.48
8k	68.16	1.98	2.91	65.74	2.01	3.05	64.88	2.22	3.42	64.06	2.10	3.28
10k	66.06	4.01	6.08	65.50	3.12	4.76	63.41	3.63	5.72	63.56	4.34	6.82
12.5k	66.66	5.98	8.97	63.94	5.30	8.29	63.37	6.11	9.64	62.89	6.13	9.75
16k	60.07	4.95	8.25	58.69	5.20	8.86	56.94	5.36	9.42	57.84	4.80	8.30
20k	52.81	3.67	6.94	52.59	3.63	6.90	49.39	4.09	8.29	50.54	3.47	6.86
NR	1	1	1	2	2	2	3	3	3	4	4	4
Min	52.81	1.45	2.16	49.93	0.78	1.56	49.39	1.49	2.22	42.11	1.12	1.57
Max	82.01	5.98	8.97	82.22	5.91	8.97	80.13	6.11	9.64	79.41	6.13	9.75

Table 5. Summary of mean values, standard deviation, and variability coefficient for microphones 5–8 for the examined frequencies.

Number of Microphones 5–8												
		5			**6**			**7**			**8**	
f [Hz]	**X**	**S**	**V**	**X**	**S**	**V**	**X**	**S**	**V**	**X**	**S**	**V**
25	68.41	3.72	5.44	82.01	4.15	5.06	79.28	4.22	5.33	75.85	5.91	7.80
31.5	58.03	2.67	4.60	62.36	2.27	3.64	57.63	3.49	6.05	62.03	2.16	3.49
40	52.85	1.19	2.25	51.68	1.01	1.95	42.84	2.92	6.81	51.92	1.03	1.98
50	73.34	1.30	1.77	61.04	3.63	5.94	62.30	2.31	3.72	61.29	1.73	2.82
63	71.39	1.94	2.71	66.06	0.61	0.92	78.21	2.21	2.82	58.88	0.74	1.26
80	65.14	1.38	2.12	64.51	2.03	3.15	67.44	1.76	2.61	67.24	1.62	2.42
100	65.03	2.00	3.08	63.06	2.26	3.58	61.91	1.52	2.45	61.11	1.40	2.30
125	70.35	3.64	5.18	68.14	3.32	4.87	66.08	1.87	2.83	68.56	2.60	3.79
160	70.10	1.61	2.30	71.53	1.77	2.47	71.57	1.56	2.17	70.61	2.36	3.34
200	73.71	5.18	7.02	80.11	5.67	7.07	76.93	3.51	4.56	74.24	4.95	6.66
250	76.27	4.05	5.31	82.66	4.71	5.69	80.56	2.44	3.03	77.23	4.37	5.65
315	75.03	3.20	4.26	71.58	2.32	3.25	74.91	2.99	3.99	68.43	3.70	5.40
400	72.09	6.20	8.60	79.24	3.50	4.42	72.39	4.29	5.93	76.61	3.54	4.63
500	73.54	6.41	8.72	80.23	3.01	3.75	73.48	4.97	6.76	77.83	4.04	5.19
630	71.31	5.20	7.29	69.24	4.11	5.93	67.73	4.91	7.25	67.98	3.36	4.95
800	65.16	2.79	4.28	65.49	2.86	4.37	66.28	2.48	3.74	64.04	2.72	4.25
1k	64.84	3.84	5.92	66.84	3.66	5.48	68.28	2.54	3.72	65.21	3.62	5.55
1.25k	68.07	2.11	3.10	68.35	2.24	3.28	67.71	2.45	3.62	67.72	2.53	3.73
1.6k	73.06	2.84	3.89	73.11	2.94	4.02	72.80	4.27	5.87	72.01	4.25	5.90
2k	72.54	3.43	4.74	74.78	3.45	4.61	74.23	3.54	4.77	73.98	3.17	4.28
2.5k	70.84	5.27	7.44	70.62	5.10	7.22	70.54	4.77	6.76	70.29	5.20	7.39
3.15k	69.31	5.08	7.33	69.79	4.73	6.78	68.26	5.17	7.58	69.09	4.91	7.10
4k	68.33	2.03	2.98	67.93	2.81	4.14	67.99	2.38	3.51	67.89	2.56	3.77
5k	64.38	1.69	2.62	63.43	1.66	2.62	64.79	2.50	3.86	63.18	1.33	2.10
6.3k	62.58	2.32	3.71	61.55	2.25	3.66	61.95	2.35	3.80	61.61	2.41	3.91
8k	64.36	1.93	2.99	64.26	1.91	2.98	63.87	1.81	2.83	64.39	1.64	2.55
10k	64.03	3.77	5.88	62.62	3.62	5.78	62.54	3.92	6.27	62.12	4.13	6.66
12.5k	62.76	5.80	9.25	60.99	5.38	8.83	61.54	5.85	9.51	62.54	6.25	10.00
16k	56.56	5.11	9.04	55.40	5.35	9.66	56.41	5.63	9.98	55.86	5.54	9.92
20k	49.07	4.31	8.78	47.76	4.55	9.54	48.76	4.07	8.35	48.43	4.54	9.38
NR	5	5	5	6	6	6	7	7	7	8	8	8
Min	49.07	1.19	1.77	47.76	0.61	0.92	42.84	1.52	2.17	48.43	0.74	1.26
Max	76.27	6.41	9.25	82.66	5.67	9.66	80.56	5.85	9.98	77.83	6.25	10.00

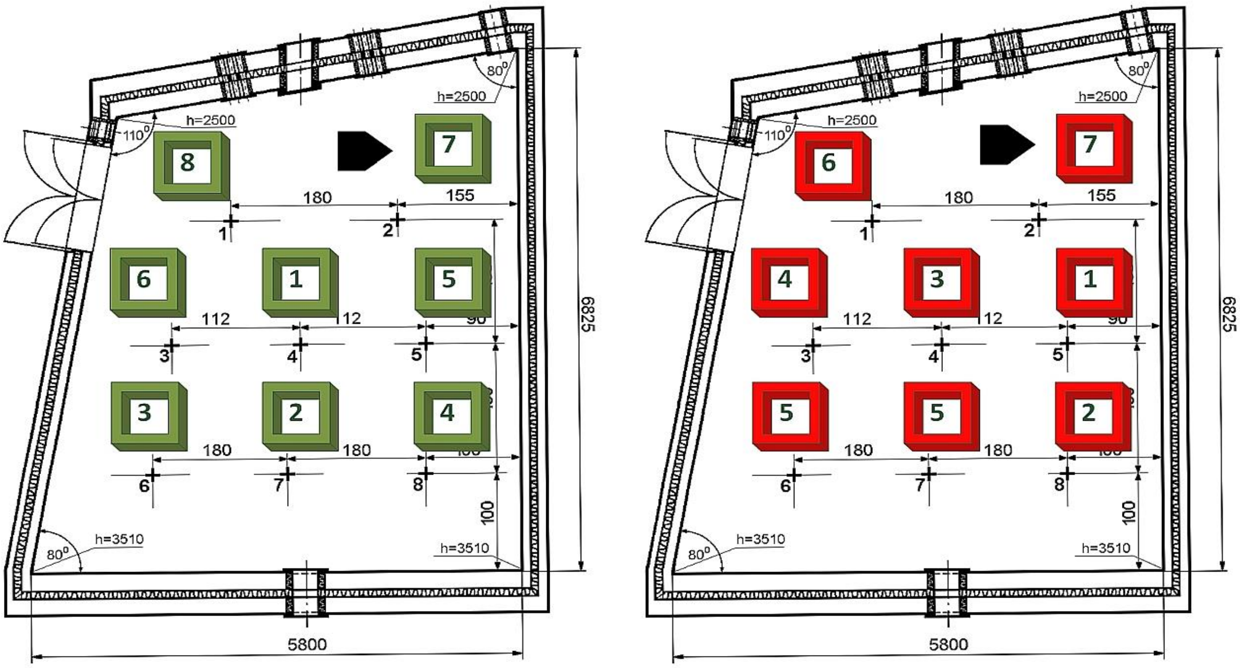

Figure 15. Analysis of mean values of registered noise.

The source values of the measured noise levels for individual ranges relative to cases are shown for the indicated microphones in Figures 16–19.

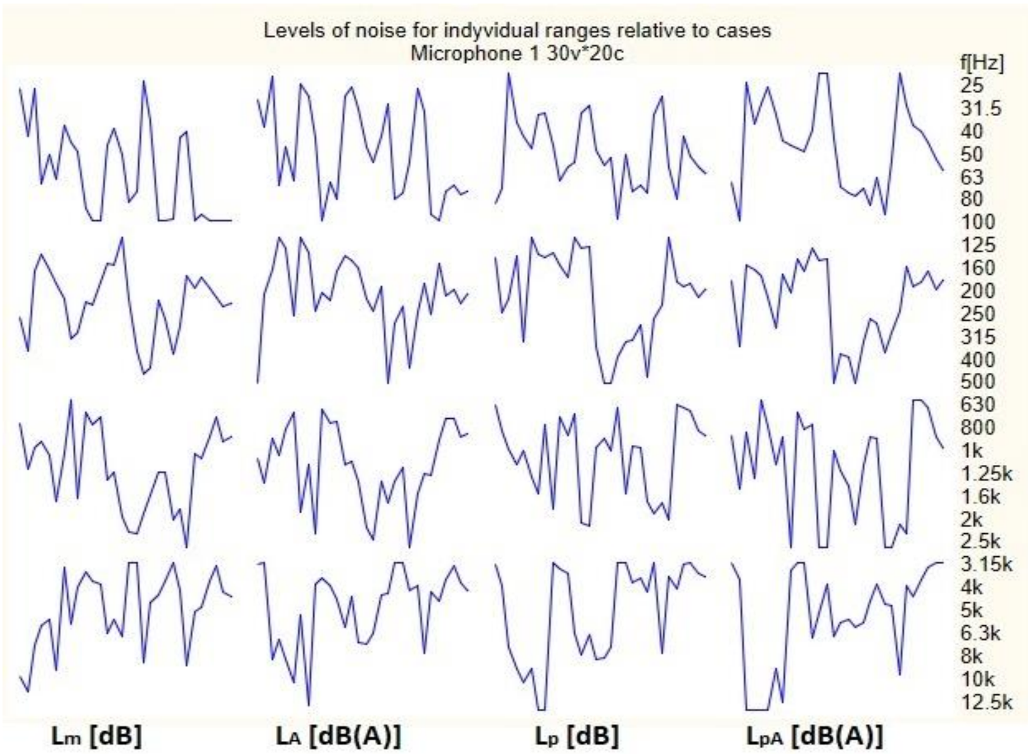

Figure 16. Source values of noise measurements for microphone 1.

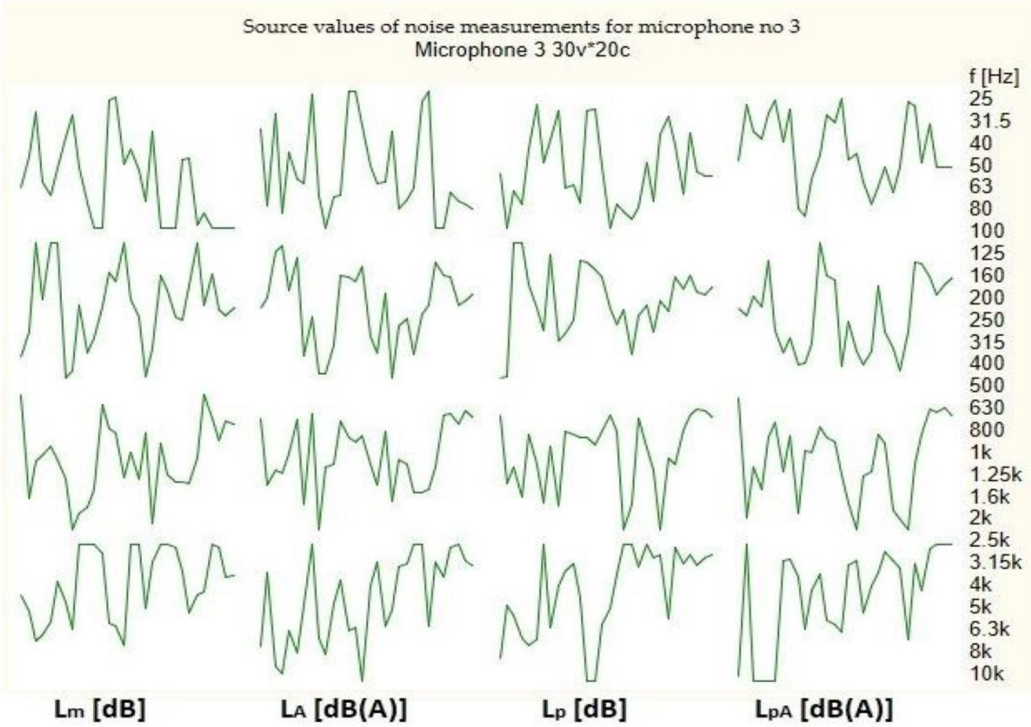

Figure 17. Source values of noise measurements for microphone 3.

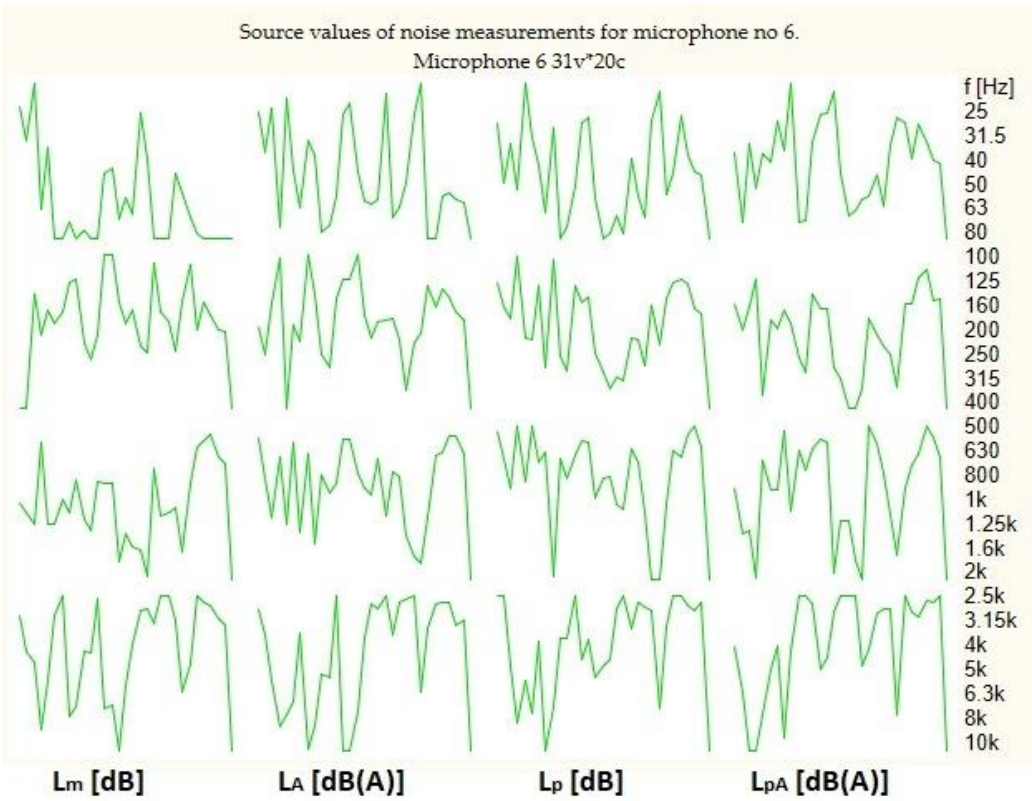

Figure 18. Source values of noise measurements for microphone 6.

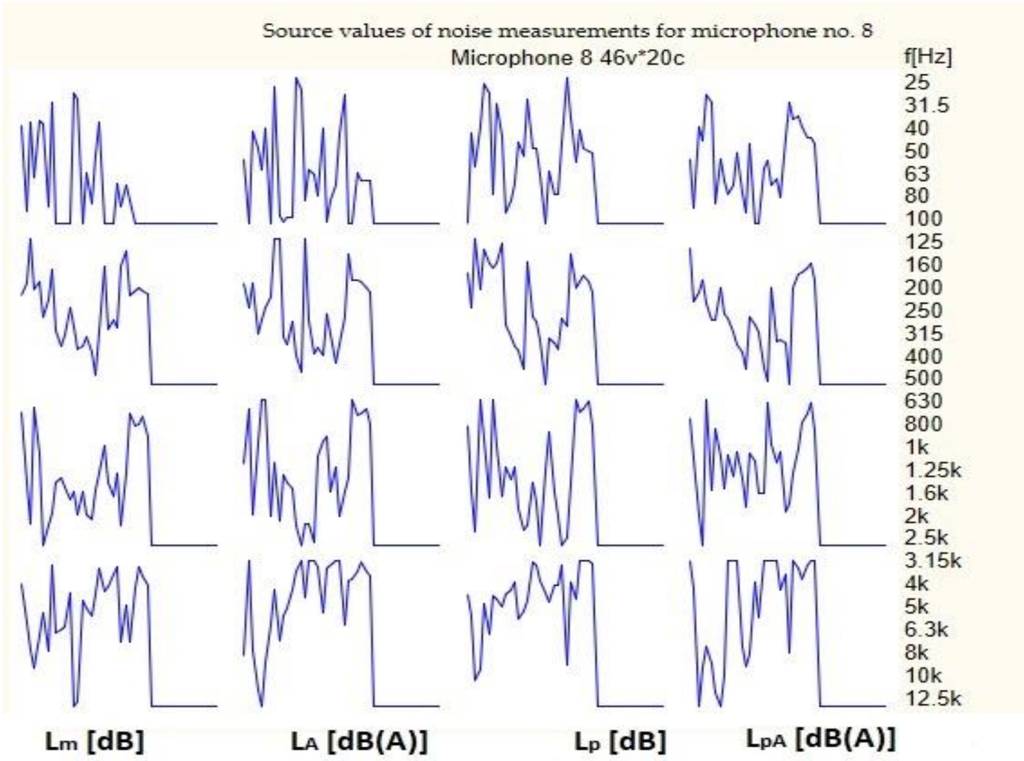

Figure 19. Source values of noise measurements for microphone 8.

Analysis of their profiles offers the visualization of the variability of individual noise values. The summary of the analysis performed is presented in Table 6.

Table 6. Analysis of the coefficient of variability.

	No.	Min	No.	Max	
1	6	0.92	1	8.97	1
2	8	1.26	2	8.97	2
3	2	1.56	5	9.25	3
4	4	1.57	3	9.64	4
5	5	1.77	6	9.66	5
6	1	2.16	4	9.75	6
7	7	2.17	7	9.98	7
8	3	2.22	8	10.00	8

When we look at the value of the standard deviation, the measurements around the average are focused on microphone 6 (Smin6 = 0.61, Smax6 =5.67). On the other hand, the values recorded with microphone 7 were found to the nearly constant: Smin7 = 1.52 and 5 Smin5 = 6.41. Moreover, we should emphasize that larger deviations are suitable for the analysis of maximum standard deviations (Table 7).

Table 7. Analysis of standard deviation.

No.	Min	Max	No.
6	0.61	5.67	6
8	0.74	5.85	7
2	0.78	5.91	2
4	1.12	5.98	1
5	1.19	6.11	3
1	1.45	6.13	4
3	1.49	6.25	8
7	1.52	6.41	5

6. Discussion

Acoustic measurements were made in a reverberation chamber in the Laboratory of Hydraulic Drives and Vibroacoustics of Machines at the Wrocław University of Technology (web site: www.lhiw.pwr.edu.pl). In chambers of this type, a perfectly diffuse field is generated. This field is characterized by the fact that all acoustic energy reflected from the walls returns in the direction of the source. This implies that the sound intensity at each point of this field is the same [41]. Based on the study of the sound field distribution, eight fixed measurement points were established in the chamber. The microphones were placed in accordance with the recommendations of the above-mentioned standards at a height of 1.3 m from the floor. The choice of the height of the microphones is related to the position of the axis of the drive shaft.

Noise generation in gear pumps has many causes and depends not only on the type of design and manufacturing technology but also on operating parameters such as the speed of the drive motor, suction and discharge pressure, oil viscosity, etc. Rotational speed and discharge pressure affect the frequency and level of oscillating force in the bearings, which creates sound-forming vibrations radiated through the housing to the environment. The suction pressure, in turn, determines the inflow conditions of the working medium. If it is too low, it can lead to the appearance of discontinuities in the jet as a result of cavitation causing an increase in the noise level in the mid- and high-frequency bands, i.e., the band in which, from the point of view of human sound perception, noise is perceived as more annoying and troublesome.

Our own research has shown the advantage of chipped wheels over ground wheels as presented in papers [42,43], among others. Additionally, an important factor is the correct selection of manufacturing tolerances and clearances. An example of this is the design with so-called zero side play, which is characterized by a 75% lower pressure pulsation. This results in a reduction of the emitted noise level by nearly 3 dB. Design parameters related to tooth geometry have a decisive influence on performance pulsation. Another important aspect is the technique of performing acoustic measurements.

The Table 8 shows an example of the results of measurements of the sound power level *Lp* and the corrected sound power level L_{pA} as a function of the discharge pressure pt and the pump shaft speed n for the analyzed experimental version of the gear pump [44].

Table 8. Sound power level *Lp* determined for a prototype pump with circumferential backlash compensation with wrap angle φ_c = 130° [42].

P_t [MPa]	n [obr/min]			
	500	1000	1600	2000
0	67.4	79.5	81.8	84.7
5	71.2	75.9	84.6	84.3
10	71.6	76.9	84.8	87.4
15	71.8	79.0	85.1	88.0
20	73.6	79.9	85.5	87.5
25	75.7	80.1	86.8	87.2
30	77.4	82.5	89.2	88.1

The paper [41] presents the waveforms of the sound value level *La* = *f*(*pt*) of gear pump 2PW-SEW-08-28-2-776. Figure 20 shows a comparison of the sound level *La* = *f*(*pt*) of gear pump 2PW-SE-08-2-77 no. 7 without side clearance, with the measurement of the hierarchic microphone being taken into account.

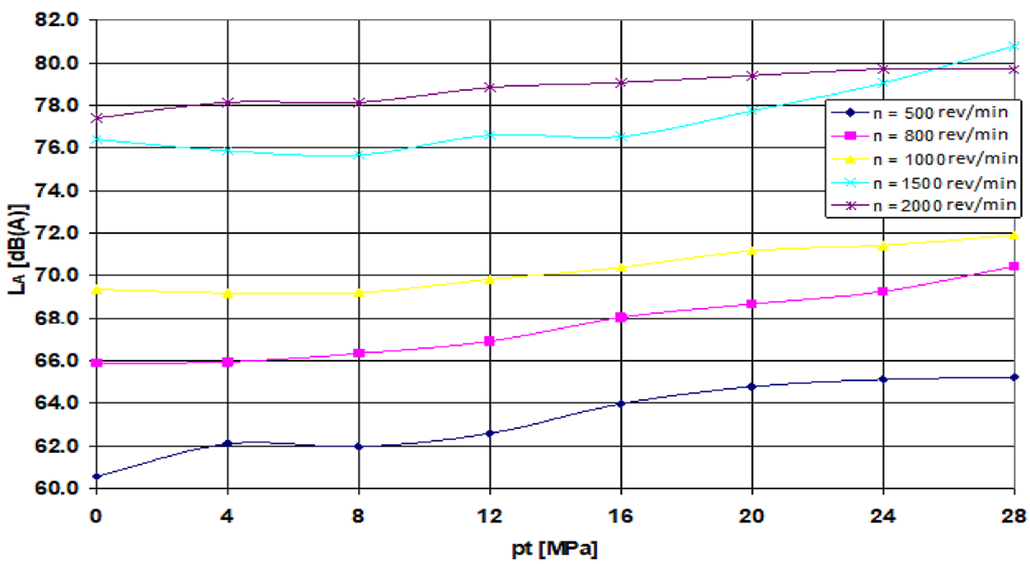

Figure 20. An example of the acoustic characteristics of a prototype pump with a three-rotor outline with ground wheels and zero lateral clearance.

The optimized method of considering the microphone signal is expected to yield better measurements of power level *Lp* and corrected sound power level *LpA* as a function of discharge pressure pt and pump shaft speed *n*.

This is of great importance in the case of turbulent flow. As the rotational velocity increases, and in turn the flow rate, the noise of the turbulent flow increases due to the greater impact of turbulence. The sound pressure level in the mid-frequency band increases by an average of 1 dB/100 rpm. The effect of turbulent flow on the increase in noise is related to the separation of the jet from the surface of the streamlined element. This phenomenon is accompanied by the appearance of varying hydrodynamic forces, which induce sound-forming vibrations of the affected surface in a direction perpendicular to the direction of flow of the working medium. In addition, the above-described phenomenon is superimposed on the effect of the noise generated inside the fluid due to mixing of fluid streams of different velocities (fluid-borne noise).

An equally important parameter affecting the characteristics of the noise emitted to the environment and associated with pressure pulsation is frequency. Due to the subjective sensation of sound impressions by humans, a reduction in speed has a beneficial effect on reducing the value of the sound level A, L_A [dB(A)]. In the modified method presented by the authors, acoustic measurement is more accurate.

7. Conclusions

The investigation conducted using induction trees reveals that the primary acoustic signal associated with the discharge pressure was detected with microphone 4. The key signal influencing the average acoustic pressure corresponded to the recording from microphone 7. The analysis demonstrates that the lowest average noise level, measuring 42.11 dB, was captured with microphone 4. As per the statistical analysis, microphone 7 held significance in the induction trees and ranked seventh in the hierarchy of minimum and maximum noise levels. This outcome suggests that the placement of microphone 7 should also undergo a comprehensive examination. To summarize the analysis, it follows that the most important element in the arrangement of microphones is the appropriate placement of microphone 4 and 7. Through the exact placement of these two measuring points, it is possible to achieve satisfactory results as if we were considering the placement of each of the microphones separately Therefore, the results of the analysis allow for one to focus on the weakest link in a set of eight microphones, which significantly reduces the research team's working time. The obtained results allowed for optimization of the number of channels in the measurement system; therefore, it is assumed that the purpose of this study has been fully achieved.

In a decision tree, tests are conducted on attribute values of examples, and the results are stored in nodes, while categories are assigned to leaves. Each possible test outcome leads to a branch connecting a node to a subtree. This enables the representation of permissible attribute values for a given set. All operations were performed in real-time during the normal operation of the gear pump. By analyzing the results obtained from the inference mechanism, which were derived from correlating continuously measured acoustic signals with model signals stored in the daB base, we identify the impact of specific microphone signals on selected parameters of the gear pump after tooth undercutting. Gear pumps belong to the family of positive displacement pumps, which are mainly used in hydrostatic drive systems. Despite many operational and utility advantages, gear pumps give way to other displacement pumps in terms of pressure pulsation and the resulting high level of emitted noise. Therefore, in order to increase the competitiveness of gear pumps, research and development work is being undertaken to reduce the noise emitted. The results of the conducted analyses indicated that the most important in the set of eight microphones is the arrangement of microphones 4 and 7. Limiting the number of measuring points will allow for the development of a data acquisition methodology based on data registration only in the indicated microphones (channels).

The conclusion of this manuscript entails the investigation of effective methods for estimating noise in gear pumps. This study contributes significantly to the field of acoustic measurements, particularly regarding the measurement of noise generated by gear pumps. The research aimed to understand the acoustic characteristics of gear pumps and identify effective measurement strategies. By employing innovative sound analysis techniques, such as time-frequency analysis and noise and vibration assessment, a better understanding of the sound characteristics produced by gear pumps and the identification of potential abnormalities in their operation were achieved. The presented results and conclusions indicate the need for further research and development of innovative measurement methods that can contribute to improving the efficiency and quality of gear pump operation. Advancements in acoustic measurements for gear pumps are crucial for optimizing design, reducing noise, and ensuring safe and efficient operation of these devices.

The result of the conducted analysis was an innovative determination of measurement points which incorporated the hierarchy of individual microphones, resulting from the classification of decision trees and statistical analysis. The obtained results allow for the optimization of the number of channels in the measurement system; therefore, it is assumed that the purpose of this study has been fully achieved.

Supplementary Materials: The following supporting information can be downloaded at: https://www.mdpi.com/article/10.3390/en16114460/s1, All Acoustic Measurement Results for All Microphones.

Author Contributions: Conceptualization, A.D. and A.M.D.; methodology, A.D. and P.O.; software, A.M.D., A.D. and P.O.; validation, P.O.; formal analysis, A.D., P.O. and A.M.D.; investigation, A.D.; resources, P.O.; data curation, A.D., P.O. and A.M.D.; writing—original draft preparation, A.D.; writing—review and editing, A.M.D.; funding acquisition, A.M.D. and P.O.; supervision, P.O. All authors have read and agreed to the published version of the manuscript.

Funding: This research received no external funding.

Data Availability Statement: Not applicable.

Conflicts of Interest: The authors declare no conflict of interest.

References

1. Xu, N.; Yu, Y.; Zhai, W.; Wang, J.; Wei, B. A high-temperature acoustic field measurement and analysis system for determining cavitation intensity in ultrasonically solidified metallic alloys. *Ultrason. Sonochemistry* **2023**, *94*, 106343. [CrossRef]
2. Fawcett, T.J.; Cooper, C.S.; Longenecker, R.L.; Walton, J.P. Machine learning, waveform preprocessing and feature extraction methods for classification of acoustic startle waveforms. *MethodsX* **2021**, *8*, 101166. [CrossRef]
3. Sause, M.G.R.; Gribov, A.; Unwin, A.R.; Horn, S.; Schull, P.J. Pattern recognition approach to identify natural clusters of acoustic emission signals. *Pattern Recognit. Lett.* **2012**, *33*, 17–23. [CrossRef]
4. Ibrahim, I.; Mohammadi, M.; Ghorbanian, V.; Lowther, D.A. Effect of Pulsewidth Modulation on Electromagnetic Noise of Interior Permanent Magnet Synchronous Motor Drives. *IEEE Trans. Magn.* **2019**, *55*, 7500805. [CrossRef]
5. Arslan, H.; Ranjbar, M.; Secgin, E.; Celik, V. Theoretical and experimental investigation of acoustic performance of multi-chamber reactive silencers. *Appl. Acoust.* **2020**, *157*, 106987. [CrossRef]
6. Ciaburro, G.; Iannace, G. Machine-Learning-Based Methods for Acoustic Emission Testing: A Review. *Appl. Sci.* **2022**, *12*, 10476. [CrossRef]
7. Su, Y.; Dong, L.; Pei, Z. Non-Destructive Testing for Cavity Damages in Automated Machines Based on Acoustic Emission Tomography. *Sensors* **2022**, *22*, 2201. [CrossRef]
8. Obaidi, S.M.A.; Leong, M.S.; Hamzah, R.I.R.; Abdelrhman, A.M. A Review of Acoustic Emission Technique for Machinery Condition Monitoring: Defects Detection & Diagnostic. *AMM* **2012**, *229–231*, 1476–1480. [CrossRef]
9. Kollek, W.; Osinski, P. *Modelling and Design of Gear Pumps*; Wydawnictwo PWr: Wroclaw, Poland, 2009.
10. Kollek, W. *Pompyzębate. Konstrukcjaieksploatacja*; Wydawnictwo Ossolineum: Wrocław, Poland, 1996.
11. Kollek, W.; Radziwanowska, U. Energetic efficiency of gear micropumps. *Arch. Civ. Mech. Eng.* **2014**, *6*, 109–115. [CrossRef]
12. Osinski, P. *Modelling and Design of Gear Pumps with Modified Tooth Profile*; Lambert Academic Publishing: Saarbrücken, Germany, 2014.
13. Osinski, P.; Kollek, W. Assessment of energetistic measuring techniques and their application to diagnosis of acoustic condition of hydraulic machinery and equipment. *Arch. Civ. Mech. Eng.* **2013**, *13*, 313–321. [CrossRef]
14. Osiński, P. *Wpływ Podcięcia Stopy Zęba na właściwości Hydrauliczne I Akustyczne Pomp Zębatych*; Raport PRE nr 14; Politechnika Wroclawska: Wroclaw, Poland, 2005.
15. Francis, J.; Betts, P.L. Modelling Incompressible Flow in a Pressure Relief Valve. *Proc. Inst. Mech. Eng.* **1997**, *211*, 83–93. [CrossRef]
16. Osiński, P.; Deptuła, A.; Partyka, M.A. Discrete optimization of a gear pump after tooth root undercutting by means of multi-valued logic trees. *Arch. Civ. Mech. Eng.* **2013**, *13*, 422–431. [CrossRef]
17. Deptuła, A.; Osiński, P. The Optimization of Three-Involute Tooth Outline with Taking into Consideration Multi-valued Logic Trees. In Proceedings of the 13th International Scientific Conference; Rusiński, E., Pietrusiak, D., Eds.; Springer International Publishing: Berlin/Heidelberg, Germany, 2017; pp. 99–107.
18. *ANSI S1.21-1972*; Methods for the Determination of Sound Power Levels of Small Sources in Reverberation Rooms. American National Standards Institute (ANSI): Washington, DC, USA, 1972.
19. *PN-85/N-01334*; Hałas—Dokładne Metody Określenia Poziomu Mocy Akustycznej Hałasu Maszyn w Komorze Pogłosowe (in Polish). Polish Committee for Standardization: Warsaw, Poland, 1985.
20. Bazan, J.G.; Nguyen, H.S.; Skowron, A.; Szczuka, M.A. View on Rough Set Concept Approximations. In *Lecture Notes in Computer Science 2639*; Wang, G., Liu, Q., Yao, Y., Skowron, A., Eds.; Springer: Chongqing, China, 2003; pp. 181–188.
21. Deptuła, A.; Partyka, M.A. Application of game graphs in optimization of dynamic system structures. *Int. J. Appl. Mech. Eng.* **2010**, *15*, 647–656.
22. Deptuła, A.; Partyka, M.A. Decision optimization of machine sets with taking into consideration logical tree minimization of design guidlines. *Int. J. Appl. Mech. Eng.* **2014**, *19*, 549–561. [CrossRef]

23. Wojcik, J.; Kostek, B. Intelligent Methods for Musical Rhythm Finding Systems. In *Intelligent Technologies for Inconsistent Knowledge Processing*; Advanced Knowledge International: Adelaide, Australia, 2004; Volume 11, pp. 1836–1841.
24. Deptuła, A.; Osiński, P.; Radziwanowska, U. Decision Support System for Identifying Technical Condition of Combustion Engine. *Arch. Acoust.* **2016**, *41*, 449–460. [CrossRef]
25. Xuo, L.; Jelinek, F. Probabilistic classification of HMM states for large vocabulary. In Proceedings of the ICASSP, Phoenix, AZ, USA, 15–19 March 1999; pp. 2044–2047.
26. Ultsch, A. Self-organising neural networks for visualisation and classifi-cation. In *Information and Classification*; Opitz, O., Lausen, B., Klar, R., Eds.; Springer: Berlin, Germany, 1993; pp. 864–867.
27. Linde, Y.; Buzo, A.; Gray, R.M. An algorithm for vector quantizer design. *IEEE Trans. Commun.* **1980**, *28*, 84–95. [CrossRef]
28. Huo-Ching, S.; Yann-Chang, H.; Chao-Ming, H. Fault Diagnosis of Power Transformers Using Computational Intelligence: A Review. *Energy Procedia* **2012**, *14*, 1226–1231.
29. Thang, K.F.; Aggrwal, R.K.; Esp, D.G.; McGrail, A.J. Statistical and Neural Network Analysis of Dissolved in Power Transformer. In Proceedings of the 2000 Eighth International Conference on Dielectric Materials, Measurements and Applications, Edinburgh, UK, 17–21 September 2000; IET: London, UK, 2000; p. 473.
30. Hong, S.I.; Ostapko, D.L. On the complementation of Boolean functions. *IEEE Trans. Comp.* **1972**, *C21*, 1022. [CrossRef]
31. Rudnik, K.; Deptuła, A.M. System with probabilistic fuzzy knowledge base and parametric inference operators in risk assessment of innovative project. *Expert Syst. Appl.* **2015**, *42*, 6365–6379. [CrossRef]
32. Deptuła, A.; Deptuła, A.M. Zastosowanie indukcyjnego system ekspertowego do procesu wyznaczania ważności kryteriów oceny ryzyka innowacyjnego. In *XLV Konferencja Zastosowań Matematyki*; Zakopane: Warswa, Poland, 2016.
33. Deptuła, A.; Deptuła, A.M. Analiza Wyników Optymalizacji Innowacyjnej Pompy Zębatej w Kontekście Ważności Zastosowanych Kryteriów Ocen. In *Innowacje w Zarządzaniu I Inżynierii Produkcji*; Knosala, R., Ed.; Oficyna Wydawnicza Polskiego Towarzystwa Zarządzania Produkcją: Opole, Poland, 2017; Volume 2, pp. 11–22.
34. Wei, W.; Liang, J.; Wang, J.; Qian, Y. Decision-relative discernibility matrices in the sense of entropies. *Int. J. Gen. Syst.* **2013**, *42*, 721–738. [CrossRef]
35. Gautam, S.; Om, H. Anomaly detection system using entropy based technique. In Proceedings of the 2015 1st International Conference on Next Generation Computing Technologies (NGCT), Dehradun, India, 4–5 September 2015; pp. 738–743. [CrossRef]
36. Li, W.; Ding, Y.; Yang, Y.; Sherratt, R.S.; Park, J.H.; Wang, J. Parameterized algorithms of fundamental NP-hard problems: A survey. *Hum. Cent. Comput. Inf. Sci.* **2020**, *10*, 29. [CrossRef]
37. Sun, B.; Chen, X.; Zhang, L.; Ma, W. Three-way decision making approach to conflict analysis and resolution using probabilistic rough set over two universes. *Inf. Sci.* **2020**, *507*, 809–822. [CrossRef]
38. Peng, Y.; Tao, Y.; Wu, B.; Wang, X. Probabilistic Hesitant Intuitionistic Fuzzy Linguistic Term Sets and Their Application in Multiple Attribute Group Decision Making. *Symmetry* **2020**, *12*, 1932. [CrossRef]
39. Pigoli, D.; Pantelis, Z.H.; Coleman, J.S.; Aston, J.A. The statistical analysis of acoustic phonetic data: Exploring differences between spoken Romance languages. *Appl. Statist.* **2018**, *67*, 1103–1145. [CrossRef]
40. Hosokawa, K.; Ogawa, M.; Hashimoto, M.; Inohara, H. Statistical Analysis of the Reliability of Acoustic and Electroglottographic Perturbation Parameters for the Detection of Vocal Roughness. *J. Voice* **2014**, *28*, 263-e9. [CrossRef] [PubMed]
41. Martin, H.R. Noise Analysis and Control in Fluid Power Systems. *Hydraul. Pneum.* **1983**, *36*, 60–64.
42. Kollek, W.; Kudźma, Z.; Maga, K.; Rutański, J.; Stosiak, M. Wpływ technologii wykonania powierzchni zębów na właściwości akustyczne i hydrauliczne pomp zębatych. *Raporty Inst. Konstr. Ekspl. Masz. PWroc.* **2007**, 37.
43. Deptuła, A.; Osiński, P.; Partyka, M.A. Analysis of Dimensional Tolerances on Hydraulic and Acoustic Properties of a New Type of Prototypal Gear Pumps. *Appl. Sci.* **2020**, *10*, 8535. [CrossRef]
44. Osinski, P. *Wysokociśnieniowe i Niskopulsacyjne Pompy Zębate o Zazębieniu Zewnętrznym*; Wydawnictwo PWr: Wroclaw, Poland, 2013.